IOPscience iopscience.iop.org

Home Search Collections Journals About Contact us My IOPscience

Identification of deep levels in GaN associated with dislocations

This article has been downloaded from IOPscience. Please scroll down to see the full text article.

2004 J. Phys.: Condens. Matter 16 6305

(http://iopscience.iop.org/0953-8984/16/34/027)

View the table of contents for this issue, or go to the journal homepage for more

Download details:
IP Address: 129.252.86.83
The article was downloaded on 27/05/2010 at 17:17

Please note that terms and conditions apply.

J. Phys.: Condens. Matter **16** (2004) 6305–6315 PII: S0953-8984(04)81489-9

Identification of deep levels in GaN associated with dislocations

C B Soh[1], S J Chua[1], H F Lim[1], D Z Chi[2], W Liu[2] and S Tripathy[2]

[1] Department of Electrical and Computer Engineering, Centre for Optoelectronics, National University of Singapore, 2 Engineering Drive 3, Singapore 117576, Singapore
[2] Institute of Materials Research and Engineering, 3 Research Link, Singapore 117602, Singapore

E-mail: elecsj@nus.edu.sg and dz-chi@imre.a-star.edu.sg

Received 29 May 2004
Published 16 August 2004
Online at stacks.iop.org/JPhysCM/16/6305
doi:10.1088/0953-8984/16/34/027

Abstract
To establish a correlation between dislocations and deep levels in GaN, a deep-level transient spectroscopy study has been carried out on GaN samples grown by metalorganic chemical vapour deposition. In addition to typical undoped and Si-doped GaN samples, high-quality crack-free undoped GaN film grown intentionally on heavily doped cracked Si-doped GaN and cracked AlGaN templates are also chosen for this study. The purpose of growth of such continuous GaN layers on top of the cracked templates is to reduce the screw dislocation density by an order of magnitude. Deep levels in these layers have been characterized and compared with emphasis on their thermal stabilities and capture kinetics. Three electron traps at E_c–E_T ∼ 0.10–0.11, 0.24–0.27 and 0.59–0.63 eV are detected common to all the samples while additional levels at E_c–E_T ∼ 0.18 and 0.37–0.40 eV are also observed in the Si-doped GaN. The trap levels exhibit considerably different stabilities under rapid thermal annealing. Based on the observations, the trap levels at E_c–E_T ∼ 0.18 and 0.24–0.27 eV can be associated with screw dislocations, whereas the level at E_c–E_T ∼ 0.59–0.63 eV can be associated with edge dislocations. This is also in agreement with the transmission electron microscopy measurements conducted on the GaN samples.

(Some figures in this article are in colour only in the electronic version.)

1. Introduction

GaN-based materials have received a great deal of attention due to their unique properties and, thus, are fast becoming established materials for wide band-gap optoelectronic devices. However, due to the lattice mismatch (of 13.5%) between GaN epilayer and the commonly used sapphire substrate [1], they inherently suffer from the drawback of having a substantially

high density of dislocations. The presence of threading dislocations, intrinsic point defects and point-defect clusters can act as non-radiative carrier recombination sites or levels reducing light-emission efficiency [2]. Besides their influence on optical performance, dislocations can act as acceptor-like centres, which can capture electrons. They can lead to the formation of defect clouds along the dislocation lines [3]. This behaviour reduces the carrier mobility due to scattering effect and could affect the performance of electronic devices, such as MOSFETs and HEMTs. The output emission from light-emitting diodes (LEDs) will also be substantially reduced as they act as diffusion channels for carriers across the p–n junctions [4]. It is therefore obvious that the formation of these dislocations as well as the electrically active defects must be minimized using optimized growth conditions and suitable starting substrates. Further reduction in the density/concentration of the dislocations related to deep levels as well as point defects can be achieved by means of postgrowth processing steps such as thermal annealing [5]. Identification of the trap levels by deep-level transient spectroscopy (DLTS) would provide more information on the characteristics and origin of the deep levels in GaN. There are variations in the assignment of deep levels in GaN [6–11] and it is the purpose of this work to identify the origin of these deep traps.

We have carried out a detailed investigation of the defects mainly by DLTS measurements of Si-doped GaN and high-quality crack-free undoped GaN grown on cracked templates. This intentional cracking at the template through the use of high Si doping GaN ($\sim 10^{19}$ cm^{-3}) or high composition of Al in AlGaN layer is aimed to relax the strain in the subsequent layers. It has been found that the screw dislocations are lowered by an order of magnitude in density on the crack-free epilayer. Three common electron traps at E_c–E_T $\sim$ 0.10, 0.24–0.27 and 0.60–0.63 eV have been detected from all the samples, while additional levels at E_c–E_T $\sim$ 0.18 and 0.37–0.40 eV have also been found in Si-doped GaN. It has been reported that the E1 deep level [6–8] with activation energy in the range 0.18–0.27 eV are associated with linear line defects along the dislocation core. However, these deep levels can originate from different sources, possibly vacancies, V_{Ga} [8–10], V_N or C impurities [11–13] or its complexes such as (V_{Ga}–O_N) [14] and (V_{Ga}–H_n) [10], which act as extended defects when decorated along dislocation lines. It is also reported that the E2 level with activation energy in the range 0.50–0.60 eV is believed to be related to the N antisite [15–17]. To understand the origin of these deep levels in the GaN samples, we have studied the effect of thermal annealing and pulse width variation by DLTS measurements, which enable their nature, such as the capture kinetics of these trap levels to be determined. Based on the experimental results, we address the origin of these trap levels in GaN.

2. Experiment

To carry out DLTS measurements, two different series of samples were grown by metalorganic chemical vapour deposition (MOCVD) on (0001)-oriented sapphire. Typical undoped and Si-doped GaN samples on LT-GaN buffer were first grown under optimized growth conditions. In addition, two sets of high-quality crack-free undoped GaN samples were intentionally grown on cracked Si-doped GaN and cracked Si-doped AlGaN templates. Trimethylgallium (TMGa) and ammonia (NH_3) were used as the source gas and SiH_4 was introduced to serve as Si dopants for the n-type layer. For the undoped and Si-doped GaN samples, the growth followed the sequence as stated below: (i) a LT-GaN buffer layer of thickness 35 nm was first deposited on sapphire at 530 °C and (ii) a 2.0-μm-thick undoped and Si-doped GaN layer of carrier concentration, $n \sim 5.0 \times 10^{16}$ and 3.0×10^{17} cm^{-3}, respectively, was grown at 1010 °C. For the high-quality crack-free GaN layer grown on cracked Si-doped GaN template, the same sources were used and the deposition procedure is based on the sequential growth of (i) a LT-GaN

buffer layer with thickness 25 nm on (0001) c-plane sapphire (Al_2O_3) substrate at 520 °C; (ii) a 1-μm-undoped GaN layer at 1020 °C; (iii) a 3 μm cracked Si-doped GaN layer ($n > 10^{19}$ cm^{-3}) at 1000 °C followed by (iv) a 1.5 μm continuous undoped GaN ($n \sim 8 \times 10^{15}$ cm^{-3}) [18]. Another set of crack-free GaN samples were grown on heavily doped cracked AlGaN templates in step (iii), where the Al composition is approximately 25%. The purpose of such growth of different sets of GaN samples on cracked template is to reduce the screw dislocation density on the top undoped GaN layer compared with the dislocation density in cracked templates. Cooling down the heavily doped GaN : Si layer induces cracks along the $\{1\bar{1}00\}$ cleavage planes. This leads to a different growth rate in different crystallographic directions for the subsequent layers resulting in a crack-free GaN layer above the cracked Si-doped GaN layer. During such a growth process, grains with larger size and lower strain have a faster growth rate and these islands will laterally overgrow the others leaving them buried. The above technique suppressed the propagation of screw dislocations to the top undoped crack-free GaN epilayer. Also, to study the deep levels in the cracked GaN : Si, the crack-free GaN film was etched to a depth of ~1.2 μm to reach the interface of cracked Si-doped GaN template. Dry etching was carried out using BCl_3/Cl_2 (20/8 sccm) plasmas at 5.0 mTorr where the rf chuck power and ICP power were 300 and 500 W, respectively.

To evaluate the thermal stabilities of these deep levels in GaN, rapid thermal annealing (RTA) was carried out in N_2 ambient at 750, 850 and 950 °C for 4 min, and the results were compared with the as-grown samples. For electrical measurements, contacts were deposited on the sample surface. In the case of the ohmic contact, Ti/Al/Pd/Au (25/220/60/160 nm) was deposited followed by rapid thermal annealing at 550 °C before the Schottky contact using Pd/Au (35/250 nm) was fabricated. A circular mask was used for lithography to deposit a circular dot pattern (of diameter 1 mm) for Schottky contact. Good I–V characteristics with low leakage current and low series resistance were observed for all the samples. The Bio-Rad DL8000 DLTS system was used for DLTS and C–V measurements, with the sample placed inside the liquid-helium cryostat. For temperature scan, DLTS spectra were obtained over a temperature range of 50–300 K. During DLTS measurements, period width t_w of 2.0 s was used under a quiescent reverse-bias voltage of −1 V and it was periodically pulsed at 2 V for trap filling. Saturated capacitance transient was obtained with a filled pulse width of 50 ms. The C–V data was used to establish the carrier profile and to ascertain that carrier concentration is much larger than the trap concentration at all temperatures. Carrier concentrations $n \sim 5.0 \times 10^{16}$, 3.0×10^{17} and 8.0×10^{15} cm^{-3} were obtained for the undoped GaN, the Si-doped GaN and the continuous undoped GaN, respectively, with trap concentrations in the range 10^{13}–10^{15} cm^{-3}. To determine the parameters of the electron traps and their capture kinetics behaviour, DLTS spectra for a set of pulse widths t_p ranging from 10^{-6} to 10^0 s were recorded.

3. Results and discussion

3.1. Characterization of high-quality crack-free undoped GaN

The properties of the crack-free GaN films on cracked Si-doped GaN have been studied by XRD and TEM. As shown in figure 1, the 2θ scan curve for $(1\bar{1}02)$ diffraction gives a narrower peak from the crack-free GaN superimposed on the broad peak from the underlying cracked Si-doped GaN, indicating the much higher crystal quality of the top continuous GaN epilayer. To get a clear picture of the layer microstructure, we have carried out transmission electron microscopy (TEM) measurements for both symmetrical and asymmetrical diffractions. Figures 2(a) and (c) show the dark-field TEM images of crack-free undoped GaN film grown on a cracked

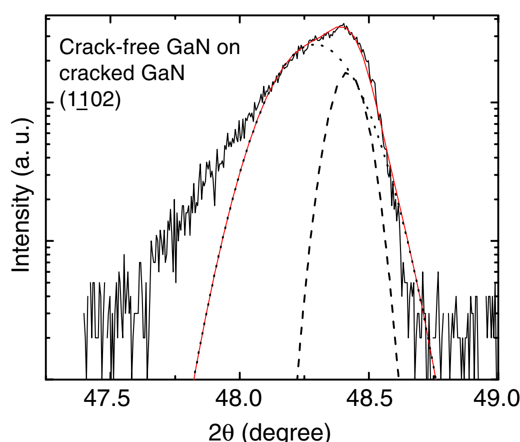

Figure 1. XRD 2θ scan for the high-quality crack-free GaN film grown on a cracked Si-doped GaN template.

Si-doped GaN template and AlGaN template, respectively. It is known that screw and/or mixed dislocations can be evaluated by symmetric diffraction measurements [19]. From the image taken along the diffraction vector (0002), dislocations in the crack-free GaN epilayer are less (by an order of magnitude) than the underlying cracked template. It appears from figure 2(a) that the dislocations near the crack are bounded together over the cracked line and hence dislocations are substantially reduced in the epilayer. Since only screw and mixed dislocations have the contrast in the dark-field image in the (0002) diffraction vector, based on figures 2(a) and 2(c), we found that screw and mixed dislocation density ($\sim 10^8$ cm^2) is greatly reduced in the epilayer compared with the cracked GaN template (where dislocation density $\sim 10^9$ cm^2). On the other hand, the reduction in dislocation density was not found in the TEM picture for the GaN epilayer taken along the ($1\bar{2}10$) diffraction vector on both Si-doped cracked GaN template and AlGaN template as shown in figure 2(b), where pure edge and mixed dislocations are visible. Since edge and mixed dislocations can be viewed from asymmetric diffraction measurements, it implies that there is no effective reduction of edge dislocation density in the crack-free GaN layer. TEM pictures confirmed that the growth technique has effectively suppressed the extent of screw dislocations, whereas edge dislocations still remain dominant in these samples. To further explore the structural properties of the crack-free GaN layers grown on cracked Si-doped AlGaN template, TEM and XRD measurements were also carried out. The TEM micrographs show a reduction of the screw dislocation density in the top high-quality crack-free undoped layer. The dislocation density in the GaN samples is also estimated using Ayer's model [20] based on the XRD linewidth and is presented in table 1.

3.2. Identification of trap levels in undoped, Si-doped and crack-free GaN

Before discussing the effectiveness of high-quality crack-free GaN in suppressing dislocation-related traps, the deep levels existing in undoped and Si-doped GaN were investigated. For the undoped GaN, three DLTS peaks A_2, A_3 and A_5 are identified as shown in figure 3(a). The detected trap levels are E_c–E_T $\sim$ 0.17 eV for A_2, E_c–E_T $\sim$ 0.24 eV for A_3 and E_c–E_T $\sim$ 0.59 eV for A_5, based on the fitting and spectral deconvolution. These observations agreed well with the results from Arrhenius plots. The ability of thermal annealing in passivating some of the defects such as vacancies and impurities decorated along the dislocation

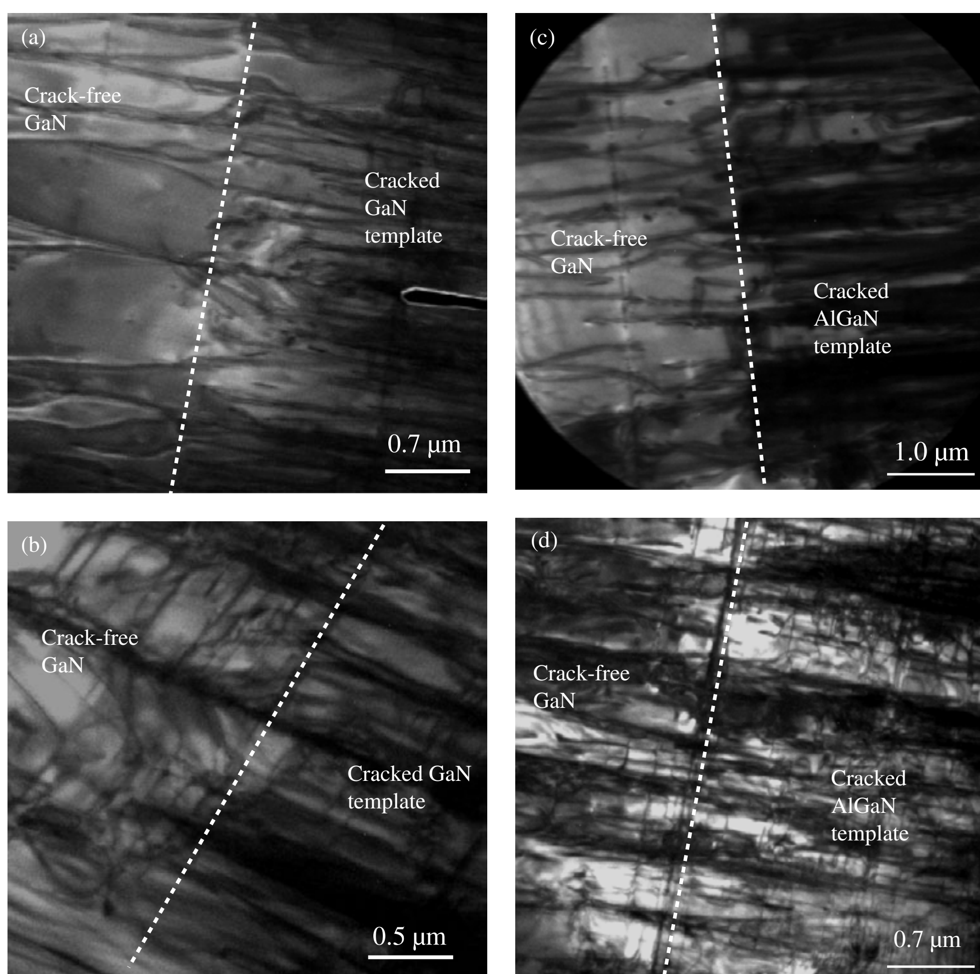

Figure 2. Dark-field TEM pictures of different areas of the continuous undoped GaN film grown on both cracked Si-doped GaN with scan taken at a diffraction vector of (a) (0002), and (b) $(1\bar{1}20)$, and AlGaN template with the scan taken at a diffraction vector of (c) (0002) and (d) $(1\bar{1}20)$.

lines were investigated in Si-doped GaN. Figure 3(b) shows the DLTS spectra measured on the as-grown and annealed Si-doped GaN. Five DLTS peaks are identified, indicating the presence of five deep-level traps before thermal annealing was carried out. The A_1 level, which has an energy position of E_c–E_T $\sim$ 0.10 eV and a trap concentration of $\sim$1.34 $\times$ 10^{13} cm^{-3}, can be related to point defects, such as the nitrogen vacancies (V_N) [21]. This deep level was also found in the undoped GaN but was not noticed due to its relatively low trap concentration. The activation energy of the donors found using Hall measurements (E_a $\sim$ 70 meV) for the Si-doped GaN can be correlated to this trap level observed by DLTS [21, 22]. The energy position as determined from the DLTS Arrhenius plot is $E_0 + \Phi_0$, where E_0 is the thermal activation energy at 0 K and Φ_0 is the energy of the capture cross-section barrier [11, 21]. Taking into account the potential barrier for electron capture, it is probable that the trap levels identified using DLTS and Hall effect measurements are of the same nature. Besides the A_1 level, four other deep-level traps A_2, A_3, A_4 and A_5 were identified with their corresponding

Table 1. (a) The trap parameters for the GaN layers determined from the Arrhenius plots. (b) Thermal stability for various defects.

(a)

Level	A_1	A_2	A_3	A_4	A_5
Undoped GaN (dislocation density $\sim 1 \times 10^9\ cm^{-2}$)					
E_c–E_T (eV)	–	0.17	0.24	–	0.59
σ_N (cm^2)	–	8.7×10^{-18}	2.6×10^{-18}	–	9.0×10^{-16}
N_T (cm^{-3})	–	3.5×10^{14}	5.5×10^{14}	–	8.5×10^{13}
Si-doped GaN (dislocation density $\sim 2.2 \times 10^8\ cm^{-2}$)					
E_c–E_T (eV)	0.10	0.18	0.24	0.40	0.62
σ_N (cm^2)	2.4×10^{-20}	7.9×10^{-18}	4.5×10^{-18}	5.2×10^{-17}	5.4×10^{-16}
N_T (cm^{-3})	1.3×10^{13}	5.5×10^{13}	8.8×10^{13}	6.9×10^{13}	9.0×10^{13}
Crack-free undoped GaN epilayer grown on cracked Si-doped GaN template (dislocation density $\sim 1.0 \times 10^8\ cm^{-2}$)					
E_c–E_T (eV)	0.11	–	0.24	–	0.63
σ_N (cm^2)	2.8×10^{-19}	–	3.4×10^{-17}	–	6.8×10^{-15}
N_T (cm^{-3})	1.1×10^{13}	–	2.0×10^{13}	–	1.0×10^{14}
Continuous undoped GaN grown on cracked Si-doped AlGaN template (dislocation density $\sim 5.0 \times 10^9\ cm^{-2}$)					
E_c–E_T (eV)	0.10	–	0.24	–	0.62
σ_N (cm^2)	3.3×10^{-19}	–	3.1×10^{-17}	–	7.2×10^{-15}
N_T (cm^{-3})	1.1×10^{13}	–	1.3×10^{13}	–	5.8×10^{13}
Cracked Si-doped GaN template (dislocation density $\sim 2.0 \times 10^9\ cm^{-2}$)					
E_c–E_T (eV)	0.11	–	0.27	0.37	0.60
σ_N (cm^2)	3.7×10^{-19}	–	8.0×10^{-16}	8.5×10^{-17}	1.3×10^{-15}
N_T (cm^{-3})	2.4×10^{13}	–	1.2×10^{14}	9.0×10^{13}	1.5×10^{14}

(b)

Origin	Nitrogen vacancies	Defect clusters along screw- and mixed-type dislocations	Si dopants-induced defects	Linear array of defects due to dangling bonds along edge dislocations
Thermal stability	750 °C	850 °C	750 °C	950 °C

energy positions at 0.18, 0.24, 0.40 and 0.62 eV, respectively. Thermal annealing at 750 °C caused the A_1 and A_4 levels to be annealed out, which suggests that they are most probably associated with the point defects. The effective reduction in DLTS signal from A_4 level enables the DLTS peak intensity due to A_5 level (with an energy position E_c–$E_T \sim 0.62$ eV) to be seen more clearly. A_5 trap level exhibits the highest thermal stability and remains stable even for an annealing temperature of 950 °C. On the other hand, the A_2 and A_3 trap levels, experience a significant drop in trap concentration under thermal annealing at 850 °C (from $\sim$0.13 to 0.02 pF). It is likely that these two levels are related to the defect clustering along mixed or screw dislocations. Further increase in the annealing temperature caused these clusters to dissociate. This leads to a decrease in the mobility as deduced from the Hall measurement data shown in figure 4. The reduction in effective screening by defect clusters can lead to stronger dislocation scattering effect, which can be expressed as

$$\mu_{dis} = C_{dis} T^x, \tag{1}$$

where x is the mobility scattering factor [23]. For as-grown Si-doped GaN, $x \sim 0.1$. Upon thermal annealing, dislocation scattering factor for the doped GaN increased to 0.18 and 0.40 for annealing at 750 and 850 °C, respectively (see inset of figure 4). This is possibly related

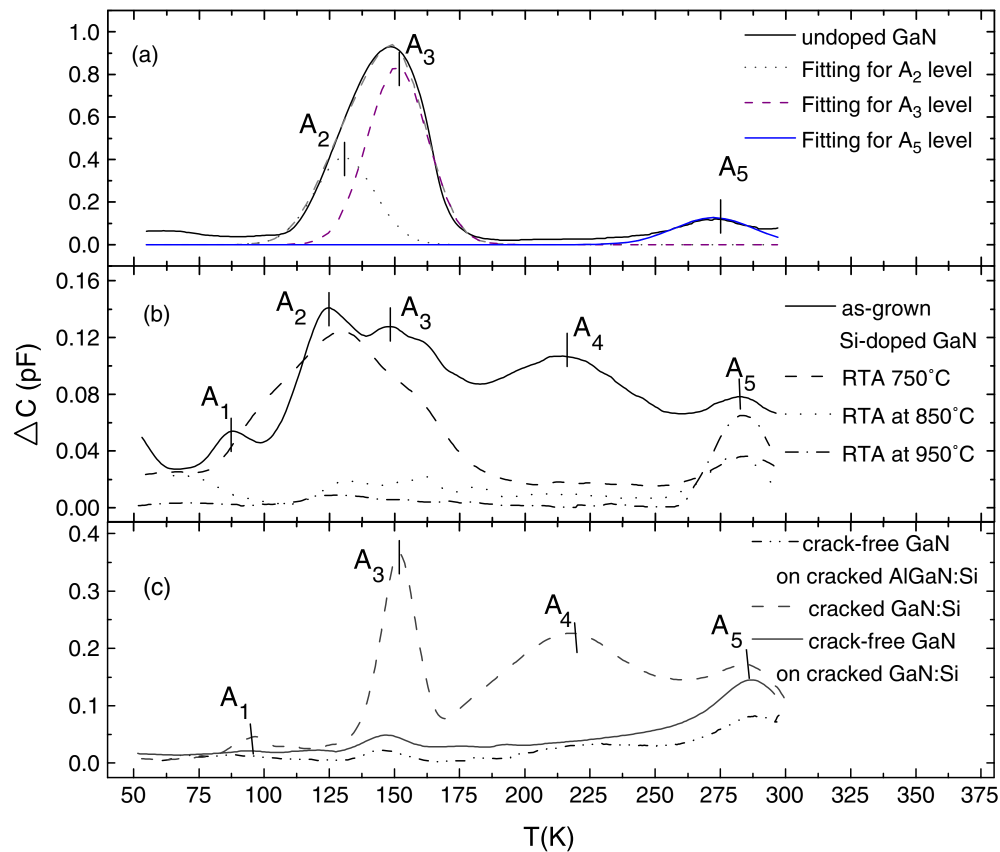

Figure 3. (a) DLTS spectra of a typical undoped GaN. (b) Effect of rapid thermal annealing on the Si-doped GaN. The DLTS measurement is performed using a period width $t_w = 2.0$ s and filling pulse width $t_p = 50$ ms at a bias, $V_r = -1.0$ V. (c) DLTS measurements carried out on the high-quality crack-free GaN film and the underlying cracked Si-doped GaN using $t_w = 2.0$ s and $t_p = 50$ ms with $V_r = -1.0$ V and $V_P = 2.0$ V.

to the dissociation of these point defects and defect clusters along screw dislocations, which enhance the dislocation scattering effect in these samples.

To investigate the origin of these trap levels, DLTS measurements have also been carried out on the crack-free undoped GaN top layer as well as on the underlying cracked Si-doped templates. The doping profile as obtained from the *C–V* measurements show that the crack-free undoped GaN top layer typically extends to a depth of $\sim$1.5 μm. Figure 3(c) shows a typical DLTS spectra of undoped crack-free GaN layers grown on both cracked Si-doped GaN and AlGaN templates. In this figure, we have also shown the DLTS spectrum for the deep levels in the cracked Si-doped GaN template, where measurements were possible due to the removal of the top crack-free GaN layer by plasma etching. It can be seen that the two GaN layers contain basically the same electron traps that were detected in Si-doped GaN sample (see figure 3(b)), except that the A_2 level is absent in both the layers and the A_4 level is reduced to noise level in the undoped crack-free GaN layer. Since the A_4 trap level is only present in Si-doped GaN, but absent in the undoped and high-quality crack-free undoped GaN layer, we can conclude that the A_4 level is associated with Si-related defects. The A_2 trap level, which is also reported by Fang *et al* [24] in electron-irradiated n-type GaN, has been attributed to N

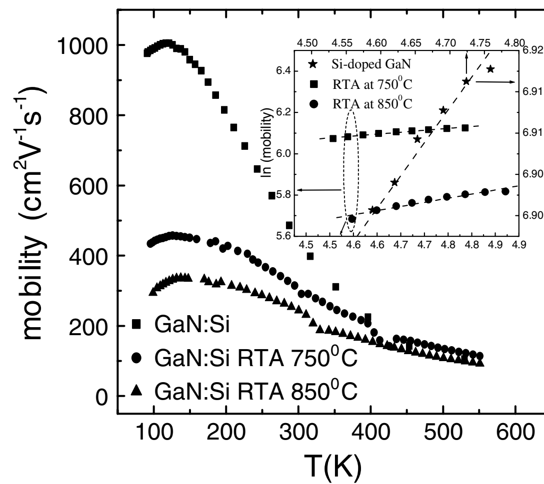

Figure 4. Plot of Hall mobility versus temperature. The inset gives the plot of ln (mobility) versus ln T for the determination of dislocation scattering effect in Si-doped GaN after thermal annealing.

vacancy (V_N). However, based on the high thermal stability for trap level A_2 as mentioned earlier, we believe that it is probably related to an extended defect structure, probably defect decoration along the dislocation site. Since the A_2 level is absent in both the crack-free undoped GaN layer on cracked Si-doped templates, it is likely that this deep level is associated with screw dislocations. Similarly, when compared with the underlying cracked GaN template, the observation of a much lower concentration of A_3 level in the top crack-free GaN layer suggests that it is associated with dislocations, as their presence has been observed to be significantly lower in the top crack-free epilayer. The A_5 level is likely related to a linear array of defects due to dangling bonds along edge dislocation based on the two experimental observations: (i) the level showed the highest thermal stability under RTA and (ii) no effective reduction of edge dislocation was observed in the top crack-free layer (see figure 2(b)). Additional experimental evidences for these assignments are presented and discussed in the following section. A summary of the trap parameters obtained from the DLTS measurements is shown in table 1. For the higher temperature (>300 K) DLTS measurements, we are expected to get emission from deeper trap levels of the band gap, for instance, the hole trap level associated with V_{Ga} at $E_v + 0.85$ eV, which plays an important role in yellow luminescence emission [25].

3.3. Capture kinetics of trap levels

The nature of the deep levels in Si-doped GaN was further examined by monitoring the dependence of A_3 and A_5 levels on filling pulse time t_p. Saturation pulse widths t_p of 1 s, 30 and 20 ms, were obtained for A_2, A_3 and A_5 levels, respectively, compared with 10 μs for the A_1 level, which is typical for a point-like defect [26]. Furthermore, the plots of peak height, ΔC, versus the filling pulse width, t_p, in figure 5 show that the magnitudes of A_2, A_3 and A_5 levels increase linearly with the logarithm of filling pulse width up to tens of milliseconds. This is an indication of the nature of trap levels associated with the extended defects [27–29]. The A_4 level has a saturation pulse time of 1.0 ms and exhibits a logarithmic capture kinetic behaviour for lower pulse width. We can attribute this level to the Si dopant, some of which

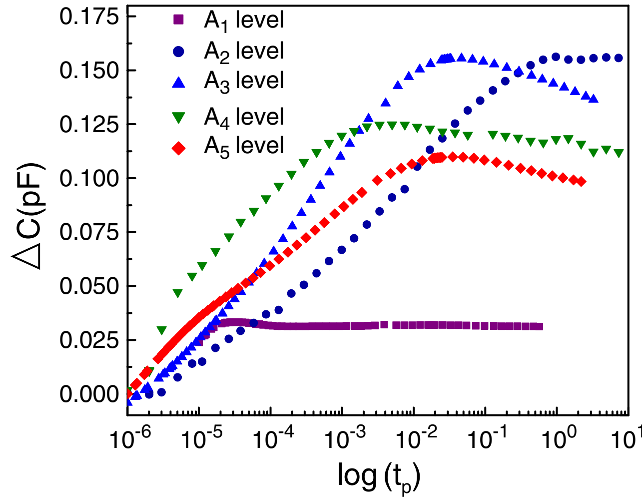

Figure 5. DLTS peak amplitude versus the filling pulse width t_p for the trap levels observed in Si-doped GaN.

may be segregated along the dislocation core sites. This accounts for its anomalous behaviour based on its low thermal stability, which is a feature of point defects. For dislocation-induced defects (attributed to either interaction between closely spaced dislocations or core sites along a particular dislocation), carrier capture depends logarithmically on the filling pulse width [26–28] and is given by the expression

$$n_T(t_p) = \sigma_n \langle \nu_n \rangle n \tau N_T \ln\left[1 + \left(\frac{t_p}{\tau}\right)\right], \tag{2}$$

where the capture time constant,

$$\tau = \left(\frac{kT}{q\Phi_0}\right)\left(\frac{n_{T0}}{N_T}\right)\left(\frac{1}{\sigma_n \langle \nu_n \rangle n}\right). \tag{3}$$

Here, Φ_0 is the time-dependent potential barrier of carrier trapping and is found to be ~50–60 meV for dislocation-related trap levels A_2, A_3 and A_5. The above results show that the deep levels A_2, A_3 and A_5 are indeed related to the linear arrays of defects due to the dangling bonds along the dislocation core sites, where charge build-up governs the capture rate. The curve will only saturate at longer filling pulses when the trap levels are effectively filled. Further increase in filling pulse width caused the trap levels to emit during the capture process, which accounts for the subsequent reduction of the DLTS peak amplitude. Based on the logarithmic capture kinetics, we can conclude that the trap levels A_2 (at E_c–$E_t \sim 0.18$ eV), A_3 (at E_c–$E_t \sim 0.24$–0.27 eV) and A_5 (at E_c–$E_t \sim 0.61$–0.63 eV) are related to extended defects. Hasse *et al* [17] and Hacke *et al* [30] have reported similar trap levels at E_c–$E_t \sim 0.60$–0.66 eV and believed that it may correspond to nitrogen antisite point defects (N_{Ga}) based on the tight-bonding theory. On the contrary, based on the logarithmic capture kinetics behaviour and its relation to the linear array of defects due to dangling bonds along edge dislocations as illustrated from TEM images of continuous crack-free undoped GaN, we can associate this deep level to extended defects.

4. Conclusions

In summary, the nature of the deep levels in GaN has been investigated with particular emphasis on the effect of rapid thermal annealing. DLTS measurements were carried out on the undoped GaN, Si-doped GaN and crack-free undoped GaN grown on cracked Si-doped GaN/AlGaN templates. A deep level at E_c–E_t ∼ 0.62 eV remains prominent after RTA at 950 °C. This coupled with its logarithmic capture kinetics behaviour led to the conclusion that it is attributed to threading dislocations, more specifically, the edge dislocations in GaN. Although deep-level traps at E_c–E_t ∼ 0.18 and 0.24–0.27 eV display a logarithmic capture behaviour, subsequent RTA treatment at 850 °C caused these deep levels to suffer a significant reduction in their trap concentration. From this behaviour, we conclude that these deep levels arise from defect clusters along screw dislocations. In addition, the decrease in Hall mobility with RTA further substantiates this observation, where less contribution from the screening effect caused by these defect clusters leads to a higher dislocation scattering effect. The E_c–E_t ∼ 0.24–0.27 eV trap levels are identified in all the samples. Based on the significant decrease in trap concentration of E_c–E_t ∼ 0.24–0.27 eV in the crack-free GaN layer grown over the underlying cracked Si-doped GaN, it is concluded that this defect level is associated with screw and mixed-type dislocations since screw dislocations are effectively suppressed in the continuous crack-free GaN epilayer. This is further confirmed by the TEM images. The defect level at E_c–E_t ∼ 0.59–0.63 eV has approximately the same trap concentration in both the crack-free and cracked Si-doped GaN templates. Therefore, the defect level at E_c–E_t ∼ 0.59–0.63 eV could be related to the linear array of defects due to dangling bonds along edge dislocations. A deep level at E_c–E_t ∼ 0.4 eV, identified in Si-doped GaN, is related to point-like defects, possibly Si_{Ga} formation since it is effectively annealed at 750 °C despite having a saturation pulse width higher than the value normally observed for point defects.

Acknowledgments

The authors would like to thank J Zhang for growing GaN layers by MOCVD.

References

[1] Pelzmann A, Mayer M, Kirchner C, Sowada D, Rotter T, Markus Kamp and Ebeling L J 1996 *MRS Int. J. Nitride Semicond. Res.* **1** 40
[2] Shi J Y, Yu L P, Wang Y Z, Zhang G Y and Zhang H 2002 *Appl. Phys. Lett.* **80** 2293
[3] Look D C and Sizelove J R 1999 *Phys. Rev. Lett.* **82** 1237
[4] Sasaoka C, Sunakawa H, Kimura A, Nido M, Usui A and Sakai A 1998 *J. Cryst. Growth* **189/190** 61
[5] Huang H Y, Chuang C H, Shu C K, Pan Y C, Lee W H, Chen W K, Chen W H and Lee M C 2002 *Appl. Phys. Lett.* **80** 3349
[6] Soh C B, Chi D Z, Lim H F and Chua S J 2001 *Proc. SPIE Int. Soc. Opt. Eng.* **4594** 211
[7] Look D C, Fang Z-Q and Polenta L 1999 *MRS Proc. Symp. on GaN and Related Alloys* vol 595, pp W10.5-1-11
[8] Hierro A, Kwon D, Ringel S A, Hansen M, Mishra U K and DenBaars S P 2000 *Appl. Phys. Lett.* **76** 3064
[9] Saarinen K *et al* 1997 *Phys. Rev. Lett.* **79** 3030
[10] Hierro A, Hansen M, Boeckl J J, Zhao L, Speck J S, Mishra U K, DenBaars S P and Ringel A 2001 *Phys. Stat. Sol.* (b) **228** 937
[11] Fang Z-Q, Look D C and Polenta L 2002 *J. Phys.: Condens. Matter* **14** 13061
[12] Ponce F A, Bour D P, Götz W and Wright P J 1996 *Appl. Phys. Lett.* **68** 57
[13] Lee I-H, Choi I H, Lee C R and Noh S K 1997 *Appl. Phys. Lett.* **71** 1359
[14] Neugebauer J and Van de Walle C C 1996 *Appl. Phys. Lett.* **69** 503
[15] Cho H K, Kim K S, Hong C-H and Lee H J 2001 *J. Cryst. Growth* **223** 38
[16] Cho H K, Kim C S and Hong C-H 2003 *J. Appl. Phys.* **94** 1485

[17] Hasse D, Schmid M, Kurner W, Dornen A, Harle V, Scholz F, Burkard M and Schweizer H 1996 *Appl. Phys. Lett.* **69** 2525
[18] Chua S J, Hao M, Zhang J and Sia E K 2001 *Phys. Stat. Sol.* (a) **188** 1, 421
[19] Metzger T *et al* 1998 *Phil. Mag.* **77** 1013
[20] Ayers J E 1994 *J. Cryst. Growth* **135** 71
[21] Castaldini A, Cavallini A and Polenta L 2000 *J. Phys.: Condens. Matter* **12** 10161
[22] Look D C, Reynolds D C, Sizelove J W, Jones R L and Molnar R J 1997 *Phys. Rev. Lett.* **79** 2273
[23] Kordos P, Morvic M, Betko J, Van Hove J M, Wowchak A M and Chow P P 2000 *J. Appl. Phys.* **88** 5821
[24] Fang Z-Q, Hernsky J W and Look D C 1998 *Appl. Phys. Lett.* **72** 448
[25] Soh C B, Chua S J, Lim H F, Chi D Z, Tripathy S and Liu W 2004 *J. Appl. Phys.* at press
[26] Omling P, Samuelson L and Grimmeiss H G 1983 *J. Appl. Phys.* **54** 5117
[27] Chatterjee B and Ringel S A 1995 *J. Appl. Phys.* **77** 3885
[28] Wosinski T 1989 *J. Appl. Phys.* **65** 1566
[29] Omiling P, Weber E R, Montelius L, Alexander H and Michel J 1985 *Phys. Rev.* B **32** 6571
[30] Hacke P, Detchprohm T, Hiramatsu K and Sawaki N 1994 *J. Appl. Phys.* **76** 304